Biochemistry and Biophysics Reports 39 (2024) 101750

Contents lists available at ScienceDirect

Biochemistry and Biophysics Reports

journal homepage: www.elsevier.com/locate/bbrep

Proof of ssDNA degraded from dsDNA for ET recombination

Yuanxia Zheng [a], Yi Zhang [a], Xuegang Li [a], Liangwei Liu [a,b,*]

[a] Life Science College, Henan Agricultural University, Zhengzhou, 450046, China
[b] The Key Laboratory of Enzyme Engineering of Agricultural Microbiology, Ministry of Agriculture, Zhengzhou, 450046, 218 Pingan Road, China

ARTICLE INFO

Keywords:
ssDNA
Isolation
phosphorothioated fluorescent dsDNA

ABSTRACT

The widely used ET recombination requires an ssDNA product degraded by Rac phage protein E588 from dsDNA for strand invasion. However, proof of the ssDNA product is still elusive. The study provided three levels of proof sequentially. The probable ssDNAs degraded by E588 from the fluorescent plus-, minus-, or double-stranded dsDNA pET28a-xylanase exhibited a half fluorescence intensity of the corresponding dsDNAs, equivalent to the E588 degradation nucleotides half that of the total nucleotides degraded from the corresponding dsDNA. The ssDNA product degraded by E588 from the fluorescent minus-stranded dsDNA was confirmed by gradient gel-electrophoresis and two nuclease degradation reactions. Degraded by E588 from the dsDNA pET28a-xylanase that had a phosphorothioated plus-stranded 5′-terminus, the plus-stranded ssDNA product was separated via gel electrophoresis and recovered via a DNAclean kit. The recovered ssDNA product was proven to have intact 5′- and 3′-ends by DNA sequencing analysis. This study provides a solid foundation for the mechanism of ssDNA invasion.

1. Introduction

For ET recombination, the Rac phage protein pairs RecE588 (E588) and RecT are used for plasmid construction, precise mutation, artificial chromosome modification, double-stranded (ds) break repair, and genome engineering [1–7]. E588 is the C-terminal 279-residue truncation that has intact 5' exonuclease activity of the 866-residue RecE known as exonuclease VIII [8,9]. Combined with the 269-residue RecT known as single-stranded (ss-) DNA binding (or annealing) protein, E588 and RecE are efficient for circular - linear and linear - linear recombination, respectively [8,10]. It is efficient for recombination of 30- to 50-bp homology arm flanked dsDNA [8,10–12], in contrast to 1000-bp homology-arm flanked dsDNA that of the recombinase RecA [13]. The C-terminal 341-residue truncation of RecE was investigated for *in vitro* recombination [14].

The mechanism of ET recombination requires an ssDNA product for strand invasion [6,15,16]. The original clues came from ssDNA-directed base mutations and fragment insertion–deletions [11,17–22]. Later clues came from ssDNA recombination targeting the lagging strand in DNA replication [2,15,16,23]. Recently, RNA-guided genome editing was performed using ssDNA-targeting Tn7-like transposase [24,25], and ssDNA-directing templates boosted the Cas9 knock-in efficiency [26]. The ssDNA product is vital for ET recombination, however, it is not directly produced from dsDNA but infers indirectly from half of the nucleotides degraded from dsDNA [9].

To prove the ssDNA product degraded from dsDNA from levels of fluoresce, separation, and DNA sequencing analysis, we amplified fluorescent (Ff-, Rf-, and Df-) and phosphorothioated fluorescent (F10sFf- or F10sRf-) dsDNA pET28a-xylanase (5851 bp) from the parental plasmid [27] (Fig. 1). The Ff-, Rf-, and Df-dsDNAs are specific for fluorescent Cy5 plus, minus, or double strands, respectively. E588 degradation of Ff-, Rf-, and Df-dsDNAs produces ssDNA and nucleotide products, amounts of which are quantified according to fluorescence intensity. The F10sFf- or F10sRf-dsDNA substrates are specific for a 10-phosphorothioate linkage plus-stranded 5′-terminus and a fluorescent Cy5 plus- or minus-strand, respectively (Fig. 1). Protected from E588 degradation, the phosphorothioated plus-stranded ssDNA can be separated via electrophoresis and recovered via a DNAclean kit. The recovered ssDNA can be confirmed via DNA sequencing analysis.

2. Materials and methods

2.1. Materials

Q5 DNA polymerase, T5 DNA exonuclease (T5exo), the nuclease *Bst*Z17I–HF (GTA*TAC) and the nuclease S1 were obtained from New

* Corresponding author.
E-mail address: liangwei@henau.edu.cn (L. Liu).

https://doi.org/10.1016/j.bbrep.2024.101750
Received 11 March 2024; Accepted 4 June 2024

England Biolabs (Beijing, China). Cy5-dATP was obtained from Thermo Fisher Scientific (Shanghai, China). Exnase II was obtained from Vazyme (Nanjing, China). The primers used were as follows: FP (CAGCCATATGATGAGTGCCG), RP (CATATGGC TGCCGCGGGCACC, with underline indicating homology arms with the primer FP), F10s (CsAsGsCsCsAsTsAsTsGsATGAGTGCCG, with "s" indicating a phosphorothioate linkage and underline indicating homology arms with the primer RP), FE (GGAGATATACATATGGATCCCG TAATCGTAGAAGA), LRE (ATGGTGCTCGAGGTCATTTGCATATTCCTT), LFV (AAGGAA TATGCAAATGACCTCGAGCACCACCACCAC), and RV (GATTACGG-GATCCATATGTATA TCTCCTTCTTAAAG). These primers were obtained from Sangon Biotech (Shanghai, China) (Table S4). The pET28a-xylanase plasmid (5851 bp) contains the *Aspergillus niger* GH11 xylanase gene at the endonucleases *Nde*I and *Xho*I [28].

2.2. Fluorescent dsDNA amplification

Linear dsDNA amplification was performed in a 50 μL volume containing 200 nM dNTPs, 10 ng of the plasmid pET28a-xylanase, 500 nmol of the primer FP, 34 nmol of the primer RP (15-fold lower than the primer FP), 0.5 U of Q5 DNA polymerase, and 1 × Q5 DNA polymerase buffer. The PCR procedure involved predenaturation at 98 °C for 3 min; 28 cycles of denaturation at 98 °C for 3 min, annealing at 72 °C for 15 s and 61 °C for 15 s; and extension at 72 °C for 205 s.

Fluorescent Ff-, Rf-, and Df-dsDNA amplification was similar except for the addition of 0.2 nM Cy5-dATP, 1000 ng of linear dsDNA template, 500 nmol of the primer FP (for Ff-dsDNA), RP (for Rf-dsDNA), or both primers (for Df-dsDNA) and 6 cycles of amplification.

2.3. Phosphorothioated dsDNA amplification

Phosphorothioated dsDNA amplification was similar except for the use of 500 nmol of the primer F10s and 34 nmol of the primer RP (15-fold lower than the primer F10s). Phosphorothioated fluorescent dsDNA amplification was similar except for the use of 1000 ng of phosphorothioated linear dsDNA template, 500 nmol of the primer F10s (for F10sFf-dsDNA) or RP (for F10sRf-dsDNA), an extra 0.2 nM Cy5-dATP, annealing at 67 °C and 56 °C, and 6 cycles of amplification.

2.4. Large-scale dsDNA production

Linear, fluorescent (Df-, Ff-, and Rf-), phosphorothioated (F10sF-), and phosphorothioated fluorescent (F10sFf-, and F10sRf-) dsDNAs were extracted on a large scale [27]. After adding 0.6 mg/ml ethidium bromide (EB) and 1.55 g/ml cesium chloride (CsCl), 3000 μL of the PCR product was equilibrated at 36,300 g by ultracentrifugation for 10 h with an Optima XE-100 (Beckman Coulter®, USA). Detected for the EB emission at 302 nm, linear, fluorescent, phosphorothioated, and phosphorothioated fluorescent dsDNA was collected by a syringe, added to an equal volume of isopropanol, centrifuged at 450 g for 3 min to remove the EB for 4 times, and purified by a DNAclean kit (Sangon Biotech, Shanghai). The linear, fluorescent (Df-, Ff-, and Rf-), phosphorothioated (F10sF-), and phosphorothioated fluorescent (F10sFf-, and F10sRf-) dsDNAs were assayed via a Nanodrop 1000 (Table S1).

2.5. E588 recombination and purification

According to the annotations of protein RecE (Swiss-prot accession number: P15032) and gene *recE* (GenBank accession number: U00096.3), the gene *E588* was amplified from one μg of *E. coli* (strain K12) genome substrates by the primers FE and LRE. The linear vector pET21a was amplified from 10 ng of the plasmid pET21a template by the primers LFV and RV. The PCR procedure was similar except for annealing at 63 °C for 15 s and 52 °C for 15 s and extension for 40 s (gene *E588*) but extension for 192 s (vector pET21a). The pET21a-*E588* plasmid was constructed by recombining the *E588* gene (50 ng) and the pET21a vector (120 ng) via Exnase II (2 μL) in a 20 μL volume at 37 °C for 30 min [29]. We transformed 10 μL of the recombinant products into 200 μL of homemade *E. coli* BL21(DE3) competent cells via a heat-shock method.

After confirmation of plasmid pET21a-*E588* accuracy by DNA sequencing analysis (Sangon Biotech, China), 2 mL of *E. coli* BL21(DE3) cells containing the accurate plasmids were transferred to 200 mL LB media. When the cells had grown to an OD_{600} of 0.6, the protein E588 was induced to be expressed by 0.4 mM of IPTG at 25 °C and 180 rpm for 8 h. The cells were collected and sonicated, and Ni^{2+}-binding resin was used to purify the protein E588 (Qiagen, China). The protein E588 had an apparent molecular mass of 35 kDa according to the SDS–PAGE assay and a 0.75 mg/ml concentration according to the Nanodrop 1000 assay.

2.6. Fluorescent dsDNA degradation

E588 degradation reaction was carried out at 37 °C for 5 h in a 10 μL volume containing 360 ng of Ff-, Rf-, or Df-dsDNA; 0.44 μg of E588; and 1 × slice buffer (500 mM Tris-HCL, 100 mM $MgCl_2$, 10 mM DTT, and 10 mM ATP). T5exo degradation was similar except for treatment with 20 U

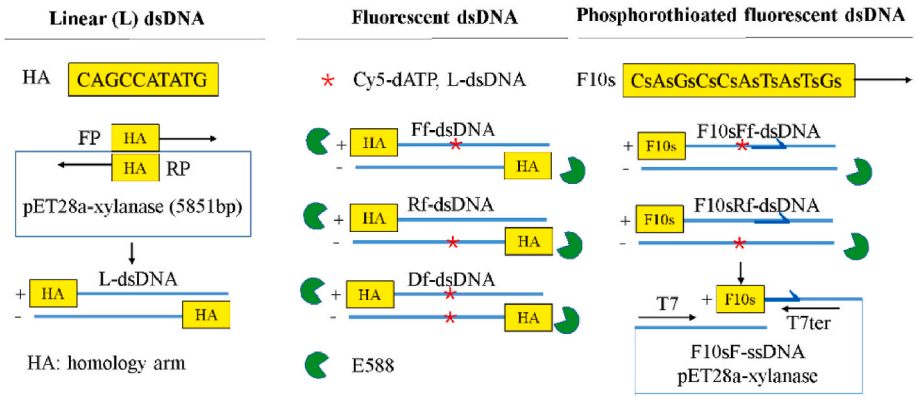

Fig. 1. Amplification and degradation of phosphorothioated fluorescent dsDNA. Amplified by the primer pair FP/RP from the parental plasmid, linear (L-) dsDNA pET28a-xylanase (5851 bp) has a10-bp homology-arm (HA) between the 5′- and 3′-terminus. Amplified from the L-dsDNA using dNTPs mixed with 1/1000 Cy5-dATP and the primer FP, RP, or both, dsDNAs are specific for fluorescent Cy5-dA plus (Ff-), minus (Rf-), or double strands (Df-) (asterisk *), respectively. Amounts of ssDNA and nucleotide products degraded by E588 ( ) from the fluorescent dsDNA are quantified by assaying fluorescence intensities. Amplified by the primer F10s that has a 5′-terminal 10 phosphorothioate linkages (with "s" indicating phosphorothioate linkage), F10sFf- or F10sRf-dsDNAs are specific for a 10-phosphorothioate linkage plus-stranded 5′-terminus and a fluorescent Cy5-dA plus- or minus-strand, respectively. Protected from E588 degradation of the F10sFf- or F10sRf-dsDNA, the phosphorothioated ssDNA can be separated via electrophoresis and recovered via a DNAclean kit, after which the ssDNA is sequenced by the primers T7 and T7ter.

of T5exos, 1 × buffer, and 37 °C for 1.5 h.

The products were diluted to a 200 μL, and was added into 400 μL of buffer P3. The mixture was filtered through a DNAclean kit to collect the filtrates; i.e., it was 600 μL of nucleotides (containing Cy5-dATP). The ssDNA was extracted in a 30 μL from the DNAclean kit. The percentage of the ssDNAs was quantified by extracting equal amounts of the Df-, Ff-, and Rf-dsDNAs via a DNAclean kit. The nucleotides and ssDNAs degraded by E588 from the Rf-dsDNAs were compared quantities directly with each other by an equivalent dilution volume of filtration and extraction via a DNAclean kit (30 μL).

2.7. Fluorescence assay

Each 4 μL of the fluorescent Ff-, Rf-, and Df-dsDNAs were added on a glass slide. Fluorescence was assayed under a laser scanning confocal microscope (A1R HD25) at a 638 nm wavelength (Nikon Corporation, Japan).

Equal amounts of the Ff-, Rf-, or Df-dsDNA substrates were degraded by T5exo or E588, and the nucleotides and the probable ssDNAs were adjusted to 200 μL and transferred to Corning 96-well round-bottom black polystyrene plates. The fluorescence intensity was assayed at 25 °C, a 30 s interval by a SpectraMax® i3x microplate reader under a 649 nm excitation wavelength and a 675 nm emission wavelength (Molecular Devices, Thermo Fisher Scientific). The fluorescence intensities of triplicate samples were averaged and statistically analysed by IBM SPSS 19 (Duncan's multiple range test ($P < 0.05$)). Figures were generated with GraphPad Prism 8 (version 8.0.2).

2.8. Gradient gel electrophoresis

Added from 1 %, 1.5 %, 2 %, to 2.5 % wt/vol gel sequentially, the gradient gel was made when the previous concentration gel solidified. Products from 720 ng of Rf-dsDNA were added to a sample well. The DNA markers used were λ-DNA *Hind* III, 50 bp ladder, DL2000, and DNA marker VI (Zoman Biotechnology, China). Gel electrophoresis was performed at 100 V for 30 min.

2.9. Redegradation of ssDNA products

E588 served to degrade 10,800 ng of Rf-dsDNAs in 30 aliquots, with each containing 360 ng of Rf-dsDNAs. The degradation products were collected, extracted from a DNAclean kit, and redegraded by the nucleases Bst171-HF and S1 at 37 °C for 2 h. The redegradation reaction mixture contained seven μL of the degradation products, 1 × CutSmart or S1 buffer, and 2 U of the nuclease Bst171-HF or S1 in a 10 μL volume. The redegraded substrates was detected via a 1.5 % wt/vol gel electrophoresis.

2.10. Separation and DNA sequencing of ssDNA products

To determine suitable degradation time,1,200 ng of the F10sRf-dsDNAs were degraded by E588 for 10, 20, 30, and 60 min. The nucleotides were filtered through a DNAclean kit and assayed for fluorescence intensity.

Based on the degradation time, 37,920 ng of F10sRf-dsDNAs or 37,200 ng of F10sFf-dsDNAs were degraded by E588 at 37 °C for 50 min, with each of the 30 aliquots contained 1200 ng of the F10sRf- or F10sFf-dsDNAs. The ssDNAs degraded from the dsDNAs was separated via a 1.5 % gel electrophoresis. A DNAclean kit was used to extract the ssDNAs. The extracted ssDNAs were DNA-sequenced by the primers T7 and T7ter (Sangon Biotech, China).

3. Results

3.1. Fluorescence evidence of the ssDNA product

Having fluorescent Cy5 plus, minus, and double strands, respectively (Fig. 1), the Ff-, Rf-, and Df-dsDNA exhibited Cy5-dA fluorescence under a laser scanning confocal microscope (Fig. S1 and Table S1). After complete degradation by T5 DNA exonuclease, the nucleotide F_Ff-, _Rf-, or _Df-T5 products degraded from the Ff-, Rf-, or Df-dsDNAs were filtered through a DNAclean kit, respectively. The nucleotide F_Df-T5 products had a twofold greater fluorescence intensity than the F_Ff- or _Rf-T5 products (Table S2), agreeing with the fact that the Df-dsDNAs had a twofold greater amount of Cy5-dA than the Ff- or Rf-dsDNAs, respectively. Amounts of the fluorescent dsDNA degradation products can be quantified by assaying fluorescence intensities.

According to the gene *recE* annotation (GenBank number: U00096.3), the recombined protein E588 had a 35 kDa apparent molecular mass agreeable with the 279 residues (Fig. S2). E588 degradation of the Ff-, Rf-, and Df-dsDNAs produced the nucleotides F_Ff-, _Rf-, and _Df-E588 and the probable ssDNA products E_Ff-, _Rf, and _Df-E588, respectively. Separated from the probable ssDNA products by DNAclean kit filtration, the nucleotides F_Ff-, _Rf-, and _Df-E588 exhibited a fluorescence intensity of 29, 21, and 67 a. u/(ng/μL), respectively (Fig. 2, and Table S2). After an equivalent amounts of the Ff-, Rf-, and Df-dsDNA substrates degraded by T5 DNA exonuclease and filtration through a DNAclean kit, the total nucleotides F_Ff-, _Rf-, and _Df-T5 F_Ff-, _Rf-, and _Df-T5 nucleotides exhibited a fluorescence intensity of 56, 39, and 133 a. u/(ng/μL), respectively (Fig. 2, and Table S2). The E588 degradation nucleotides F_Ff-, _Rf-, and _Df-E588 had a 53 %, 53 %, and 50 % percentage to the corresponding total degradation nucleotides

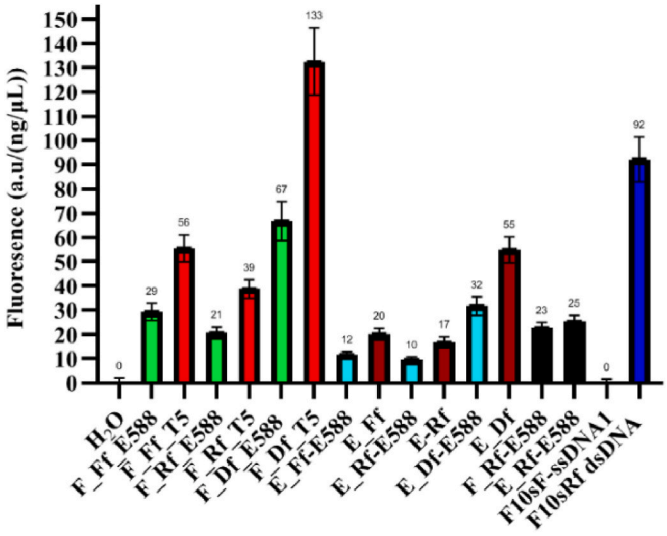

Fig. 2. Fluorescence intensities of the nucleotide and ssDNA products degraded from fluorescent dsDNA. H_2O: blank control of water; Ff-, Rf-, and Df-dsDNA: fluorescent dsDNA had the specific Cy5-dA plus (Ff-), minus (Rf-), and double strands (Df-). Nucleotide and ssDNA products degraded by E588 and T5 DNA exonuclease from an equal amount of the fluorescent dsDNA substrates were filtered and extracted from a DNAclean kit. F_Ff-, _Rf-, and _Df-E588: nucleotides degraded by E588 from the Ff-, Rf-, and Df-dsDNA substrates, respectively; F_Ff-, _Rf-, and _Df-T5: total nucleotides degraded by T5 DNA exonuclease from the Ff-, Rf-, and Df-dsDNA substrates, respectively; E_Ff-, _Rf-, and _Df-E588: ssDNAs degraded by E588 from the Ff-, Rf-, and Df-dsDNAs, respectively; E_Ff, _Rf, and _Df: equal amounts of the Ff-, Rf-, and Df-dsDNAs extracted from a DNAclean kit, respectively; F_ and E_Rf-E588: nucleotide and ssDNA products degraded by E588 from the Rf-dsDNA were filtered and extracted by an equivalent volume of dilution, respectively; F10sF-ssDNA1 and F10sRf-dsDNA: F10sF-ssDNA and the leftover dsDNA degraded by E588 from the phosphorothioated fluorescent F10sRf-dsDNA were extracted from gel electrophoresis.

F_Ff-, _Rf-, and _Df-T5, respectively. Half of the nucleotides degraded by E588 from the fluorescent dsDNA substrates indicated half of the remaining products to be ssDNA. These results agreed with half of nucleotides degraded by exonuclease VIII from dsDNA [9].

Extracted from DNAclean kit, the probable ssDNAs E_Ff-, _Rf-, and _Df-E588 degraded by E588 from the Ff-, Rf-, and Df-dsDNAs exhibited a fluorescence intensity of 12, 10, and 32 a. u/(ng/μL), respectively (Fig. 2 and Table S2). Extracted from a DNAclean kit, an equal amount of the Ff-, Rf-, and Df-dsDNAs exhibited a fluorescence intensity of 20, 17, and 55 a. u/(ng/μL), respectively (Fig. 2 and Table S2). The probable ssDNAs E_Ff-, _Rf-, and _Df-E588 had a 57 %, 57 %, and 58 % percentage of the equal amount extracted Ff-, Rf-, and Df-dsDNAs, respectively. The results showed that E588 degradation of the dsDNA substrates produced half of the probable ssDNAs.

Instead of quantifying percentage to the respective total nucleotides and the dsDNAs, the nucleotide F_ Rf-E588 and the ssDNA E_Rf-E588 degraded by E588 from the Rf-dsDNAs were compared directly with each other. After filtration and extraction from a DNAclean kit by an equivalent volume of dilution, the F_ Rf-E588 and the E_Rf-E588 products exhibited almost an equivalent fluorescence intensity (23 vs 25 a. u/(ng/μL)) (Fig. 2 and Table S2). E588 degradation of the Rf-dsDNAs produced an equal amount of the nucleotide and the ssDNA products, indicating half of the ssDNA products.

Fluorescence assay showed that E588 degradation of the fluorescent dsDNAs produced half of the ssDNAs, half of the nucleotides, and an equal amount of the two products. The results indicated that half of the ssDNA product was degraded from the dsDNA substrates.

3.2. Gradient gel-electrophoresis of the ssDNA product

The fluorescence assay indicated that E588 degradation of the fluorescent dsDNA produced half of the ssDNAs. However, gel electrophoresis separated none of the ssDNAs (Fig. S3). The ssDNAs might be degraded from both strands into different sizes. This hypothesis was validated by a gradient gel electrophoresis of the ssDNAs degraded by E588 from the Rf-dsDNAs. The ssDNAs got together at the 1 %–1.5 % gel junction (Fig. S4). Extracted from the gel junction via a DNAclean kit, the ssDNA (E_Rf-E588-Gel) exhibited a fluorescence intensity of 11.7 a. u/(ng/μL) (Table S2), agreeing with the fluorescent minus-strand. However, the minus and plus ssDNAs could not separate from each other.

3.3. Nuclease degradation of the ssDNA product

To validate if it was ssDNA or not, the ssDNAs degraded by E588 from the fluorescent Rf-dsDNAs were redegraded by the nuclease Bst171-HF and the nuclease S1 [30]. The Bst171-HF reaction produced a band corresponding to the ssDNAs and two bands corresponding to the 2699- and 3087-bp fragments (Fig. S5), showing that the nuclease Bst171-HF did not degrade the ssDNA. The nuclease S1 reaction did not reveal an ssDNA band (Fig. S5), showing degradation of the ssDNAs. The two reactions confirmed the ssDNA products to be ssDNA, agreeing with the finding of the nuclease S1 degradation [9].

3.4. Separation evidence of the ssDNA product

Fluorescence and gradient gel electrophoresis indicated that ssDNA was generated from both strands of the dsDNA, agreeing with the RecET symmetric degradation of dsDNAs [16]. Separation of ssDNA is needed to protect its 5′-terminus from E588 degradation. A phosphorothioate linkage was 100-fold more stable than a phosphodiester bond [31–33]. Therefore, the F10sRf-dsDNAs were amplified to have a 10-phosphorothioate linkage plus-stranded 5′-terminus and a fluorescent minus-strand (Fig. 1).

The fluorescent minus-strand served to determine a suitable degradation time for leaving the phosphorothioated F10sF-ssDNA intact. After E588 degradation for 10–60 min and DNAclean kit filtration, the 50 min degradation nucleotides exhibited a 69 % fluorescence intensity of the minus-strand total nucleotides (Fig. S6). A 50-min E588 degradation reaction was suitable for producing phosphorothioated F10sF-ssDNA (Fig. S7).

According to the 50-min degradation assay, 37,920 ng of the F10sRf-dsDNA was degraded by E588. Gel electrophoresis of the degradation products separated the F10sF-ssDNAs at the 2900 bp position, almost half that of the 5851 bp F10sRf-dsDNAs (Fig. 3). Extracted via a DNAclean kit, the F10sF-ssDNA1 products had a 17.3 ng/μL concentration. The product did not exhibit fluorescence; agreeing with the nonfluorescent plus-strand (Fig. 2 and Table S1). Extracted via a DNAclean kit, the remaining F10sRf-dsDNAs had a 92.2 a. u/(ng/μL) fluorescence intensity, agreeing with the fluorescent minus-strand (Fig. 2 and Table S2). The results indicated the separated F10sF-ssDNA1 products to be ssDNA.

To evaluate the phosphorothioate protection further, E588 degraded 37,200 ng of the F10sFf-dsDNAs that had a 10-phosphorothioate linkage plus-stranded 5′-terminus and a fluorescent plus-strand (Fig. 1). Gel electrophoresis of the degradation products revealed a similar F10sF-ssDNA2 product (Fig. S8). Extracted via a DNAclean kit, the F10sF-ssDNA2 product had a concentration of 11.4 ng/μL. The product had a fluorescence intensity of 305.6 a. u/(ng/μL), agreeing with that of the fluorescent plus-strand (Tables S1 and S2). Extracted via a DNAclean kit, the remaining F10sFf-dsDNAs exhibited a fluorescence intensity of 225.7 a. u/(ng/μL) (Table S2).

3.5. Sequencing evidence of the ssDNA product

Fluorescence, nuclease S1 degradation, and separation assays confirmed the ssDNA degraded by E588 from dsDNA. A direct proof would be a DNA sequencing analysis of the separated F10sF-ssDNA1 product. Located in reliable distance of DNA sequencing analysis, the F10sF-ssDNA1 3′- and 5′-termini were 119 bp downstream of the primer T7 and 623 bp upstream of the primer T7ter, respectively (Fig. 1). DNA sequencing analysis revealed that the F10sF-ssDNA1 product had intact 3′- and 5′-ends (Fig. 3); i.e., E588 degradation of the F10sRf-dsDNA produced an intact ssDNA product.

The primer T7 DNA sequencing analysis showed that the F10sF-ssDNA1 3′-terminus was CAGCCATATG, and the homology arm was also the F10sF-ssDNA1 5′-terminus (strictly speaking, the sequence should be CsAsGsCsCsAsTsAsTsGs, with “s” indicating a phosphorothioate linkage) (Fig. 1). However, the 5′-terminal sequencing signal was lower than usual. The F10sRf-dsDNAs were DNA-sequenced to determine the reliability of the lower-than-usual sequencing signal (Fig. S9). The 5′-terminal sequencing signal of F10sRf-dsDNA was also lower than usual, indicating the reliability of the 5′-terminal DNA sequencing signal of F10sF-ssDNA1.

The F10sF-ssDNA2 product was also DNA-sequenced via the primers T7 and T7ter. The results showed that the F10sF-ssDNA2 product also had intact 3′- and 5′-ends (Fig. S8). The 5′-terminal sequencing signal was also lower than usual but consistent with that of the F10sFf-dsDNAs (Fig. S10). The lower-than-usual sequencing signal might be due to the 10-phosphorothioate plus-stranded 5′-terminus, which interferes with DNA amplification during DNA sequencing analysis.

4. Discussion

To prove ssDNA degraded from dsDNA is vital for the application and investigation of ET recombination [2,6,16,23]. We proved the ssDNA product from three levels of evidence. E588 degradation of the fluorescent Ff-, Rf, and Df-dsDNAs produced an equal amount of the ssDNA and nucleotide product, with the former having half fluorescence intensity of the dsDNAs and the latter half that of the total degradation nucleotides. Equal amounts of the two degradation products, gradient gel electrophoresis and redegradation of the ssDNAs via the Bst171-HF

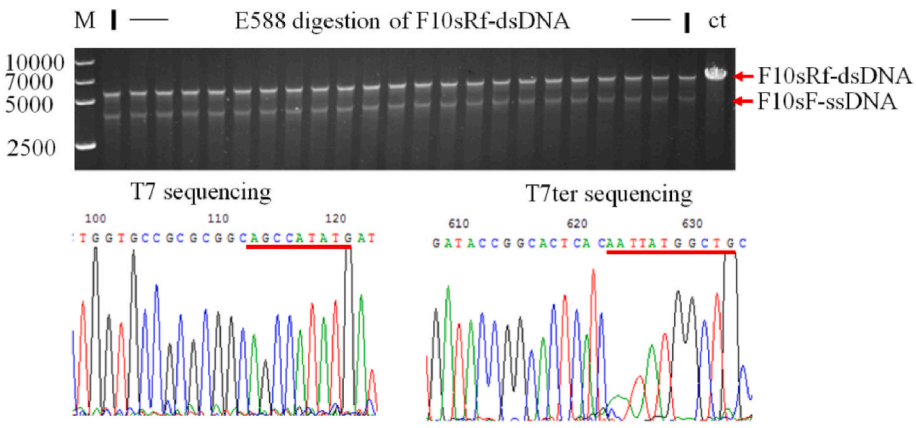

Fig. 3. Gel electrophoresis and DNA sequencing of the plus-stranded F10sF-ssDNAs. Gel electrophoresis (top) separated the phosphorothioated F10sF-ssDNA degraded by E588 from the phosphorothioated fluorescent F10sRf-dsDNA (the arrow), M: DNA marker VI, ct: control of the 5851-bp dsDNAs. The primer T7 and T7ter DNA sequencing analysis (bottom) showed that the separated F10sF-ssDNA products had intact 3′- and 5′-ends (the underline).

and S1 nucleases proved the ssDNA degraded from dsDNA. Furthermore, E588 degradation of the phosphorothioated dsDNAs separated the plus-stranded F10sF-ssDNA product. The product was proven to have the intact 5′- and 3′-ends. Direct proof of the ssDNA product provided a solid foundation for the strand invasion mechanism. The results were agreeable with that half of the nucleotides were degraded from the radio-labeled dsDNA [9].

The specific fluorescent plus-, minus-, or double-stranded dsDNAs used differ from unspecific radio-labeled and PicoGreen-dyed dsDNAs [9,34,35]. The fluorescence intensity of the dsDNA can be adjusted by the ratio of Cy5-dATP to dNTPs according to the size of the target dsDNA and the base dA content of strand. The fluorescent dsDNA, degradation nucleotides, and ssDNA can be quantified by assaying fluorescence intensities (Table S2). The fluorescence intensity was affected the least by the nucleotides, intermediately by the duplex dsDNAs, and the most strongly by the complicated ssDNAs. According to the 50-min degradation time assay (Fig. S6), E588 degraded F10sRf-dsDNA at 17.1 nucleotides/s, similar to the 18.8 nucleotides/s degradation rate of the E564 truncation [34], and faster than the 12 nucleotides/s degradation rate of Redα [36]. E588 degraded the ten phosphorothioate F10sFf-ssDNA and had a 16.0 a. u/(ng/μL) fluorescence intensity (Table S3), agreeing with that the dsDNAs phosphorothioated at both 5′-termini exhibited an increased recombination efficiency [2,15,23]. The F10sFf-ssDNA product had a smaller apparent molecular mass than the phosphorothioated dsDNA (Fig. 3 and S8), agreeing with that 12-bp dsDNA has a larger molecular mass and an almost twofold greater magnitude circular dichroism (CD) spectrum than does its counterpart ssDNA [37–39].

We separated the phosphorothioated F10sF-ssDNA product by an *in vitro* DNA phosphorothioation, which is also an *in vivo* DNA protection mechanism [33,40]. Hydroxylation might be another *in vivo* DNA protection mechanism. Redα degrades phosphoryl- but not hydroxyl-dsDNAs [23], while RecE degrades both phosphoryl- and hydroxyl-dsDNAs [9]. The general DNA protection *in vivo* might be ssDNA-binding proteins, such as Redβ [41], RecT [42], and *Salmonella enterica* SSB [43]. The L. *innocua* RecT binds to 5 bp of DNA [42]. Redβ cannot replace RecT for *in vivo* recombination of ET, and *vice versa*. Redα interacts via hydrophobic and trimeric interactions with three copies of the Redβ C-terminal domain [41]. RecE or E588 should interact in tetramers with four copies of RecT for recombination [9,34]. The C-terminal truncation E606 had a 10 Å wide and 40 Å deep toroidal channel as a tetramer to degrade dsDNA instead of ssDNA [34].

Funding

This work was supported by the National Natural Science Foundation of China (31,771,915).

CRediT authorship contribution statement

Yuanxia Zheng: Data curation. **Yi Zhang:** Data curation. **Xuegang Li:** Data curation. **Liangwei Liu:** Conceptualization.

Declaration of competing interest

The authors declare that there is not conflict of interest in the paper.

Data availability

Data will be made available on request.

Appendix A. Supplementary data

Supplementary data to this article can be found online at https://doi.org/10.1016/j.bbrep.2024.101750.

References

[1] J. Muyrers, Y. Zhang, G. Testa, A.F. Stewart, Rapid modification of bacterial artificial chromosomes by ET-recombination, Nucleic Acids Res. 27 (1999) 1555–1557.
[2] J. Mosberg, M.J. Lajoie, G.M. Church, Lambda Red recombineering in *Escherichia coli* occurs through a fully single-stranded intermediate, Genetics 186 (2010) 791–799.
[3] J. Yang, B. Sun, H. Huang, Y. Jiang, L. Diao, B. Chen, C. Xu, X. Wang, J. Liu, W. Jiang, S. Yang, High-efficiency scarless genetic modification in *Escherichia coli* by using lambda red recombination and I-SceI cleavage, Appl. Environ. Microbiol. 80 (2014) 3826–3834.
[4] A. Bird, A. Erler, J. Fu, J.-K. Hériché, M. Maresca, Y. Zhang, A. Hyman, A. Stewart, High-efficiency counterselection recombineering for site-directed mutagenesis in bacterial artificial chromosomes, Nat. Methods 9 (2012) 103–109.
[5] S.D. Hall, R.D. Kolodner, Homologous pairing and strand exchange promoted by the *Escherichia coli* RecT protein, Proc. Natl. Acad. Sci. U.S.A. 91 (1994) 3205–3209.
[6] P. Noirot, R.D. Kolodner, DNA strand invasion promoted by *Escherichia coli* RecT protein, J. Biol. Chem. 273 (1998) 12274–12280.
[7] H. Huang, X. Song, S. Yang, Development of a RecE/T-assisted CRISPR-cas9 toolbox for *lactobacillus*, Biotechnol. J. 14 (2019) e1800690.
[8] Y. Zhang, F. Buchholz, J. Muyrers, A. Stewart, A new logic for DNA engineering using recombination in *Escherichia coli*, Nat. Genet. 20 (1998) 123–128.
[9] J. Joseph, R. Kolodner, Exonuclease VIII of *Escherichia coli*,II mechanism of action, J. Biol. Chem. 258 (1983) 10418–10424.
[10] J. Fu, X. Bian, S. Hu, H. Wang, F. Huang, P. Seibert, A. Plaza, L. Xia, R. Muller, A. Stewart, Full-length RecE enhances linear-linear homologous recombination and facilitates direct cloning for bioprospecting, Nat. Biotechnol. 30 (2012) 440–446.
[11] H. Wang, Z. Li, R. Jia, Y. Hou, J. Yin, X. Bian, A. Li, R. Müller, A.F. Stewart, J. Fu, Y. Zhang, RecET direct cloning and Redab recombineering of biosynthetic gene clusters, large operons or single genes for heterologous expression, Nat. Protoc. 11 (2016) 1175–1190.

[12] H. Wang, Z. Li, R. Jia, J. Yin, A. Li, L. Xia, Y. Yin, R. Muller, J. Fu, A. Stewart, Y. Zhang, ExoCET: exonuclease in vitro assembly combined with RecET recombination for highly efficient direct DNA cloning from complex genomes, Nucleic Acids Res. 46 (2018) 5e28.
[13] Q. Lu, Seamless cloning and gene fusion, Trends Biotechnol. 23 (2005) 199–202.
[14] Y. Zhu, X. Han, Y. Niu, B. Zheng, X. Li, Q. Xu, P. Chen, Recombinant expression of truncated exonuclease VIII and its application in in vitro DNA recombination, Chin. J. Biotechnol. 35 (2019) 827–836.
[15] J. Mosberg, C.J. Gregg, M.J. Lajoie, H.H. Wang, G.M. Church, Improving lambda Red genome engineering in *Escherichia coli* via rational removal of endogenous nucleases, PLoS One 7 (2012) e44638.
[16] L. Thomason, N. Costantino, D.L. Court, Examining a DNA replication requirement for bacteriophage λ Red- and Rac prophage RecET-promoted recombination in *Escherichia coli*, mBio 7 (2016) e01443, 01416.
[17] H. Ellis, D. Yu, T. DiTizio, D.L. Court, High efficiency mutagenesis, repair, and engineering of chromosomal DNA using single-stranded oligonucleotides, Proc. Natl. Acad. Sci. U. S. A 98 (2001) 6742–6746.
[18] Y. Zhang, J.P. Muyrers, J. Rientjes, A.F. Stewart, Phage annealing proteins promote oligonucleotide-directed mutagenesis in *Escherichia coli* and mouse ES cells, BMC Mol. Biol. 4 (2003) 1.
[19] S. Sharan, L.C. Thomason, S.G. Kuznetsov, D.L. Court, Recombineering: a homologous recombination-based method of genetic engineering, Nat. Protoc. 4 (2009) 206–222.
[20] J. Fu, M. Teucher, K. Anastassiadis, W. Skarnes, A.F. Stewart, A recombineering pipeline to make conditional targeting constructs, Methods Enzymol. 477 (2010) 125–144.
[21] L. Thomason, J.A. Sawitzke, X. Li, N. Costantino, D.L. Court, Recombineering: genetic engineering in bacteria using homologous recombination, Curr. Protoc. Mol. Biol. 106 (2014) 1e30.
[22] G. Pines, E.F. Freed, J.D. Winkler, R.T. Gill, Bacterial recombineering: genome engineering via phage-based homologous recombination, ACS Synth. Biol. 4 (2015) 1176–1185.
[23] M. Maresca, A. Erler, J. Fu, A. Friedrich, Y.M. Zhang, A.F. Stewart, Single-stranded heteroduplex intermediates in λ Red homologous recombination, BMC Mol. Biol. 11 (2010) 54.
[24] J. Strecker, A. Ladha, Z. Gardner, J.L. Schmid-Burgk, K.S. Makarova, E.V. Koonin, F. Zhang, RNA-guided DNA insertion with CRISPR-associated transposases, Science 365 (2019) 48–53.
[25] S.E. Klompe, P. Vo, T. Halpin-Healy, S. Sternberg, Transposon-encoded CRISPR–Cas systems direct RNA-guided DNA integration, Nature 571 (2019) 219–225.
[26] B. Shy, V. Vykunta, A. Ha, A. Talbot, T. Roth, D. Nguyen, W. Pfeifer, Y. Chen, F. Blaeschke, E. Shifrut, S. Vedova, M. Mamedov, J.-Y.J. Chung, H. Li, R. Yu, D. Wu, J. Wolf, T. Martin, C. Castro, L. Ye, J. Esensten, J. Eyquem, A. Marson, High-yield genome engineering in primary cells using a hybrid ssDNA repair template and small-molecule cocktails, Nat. Biotechnol. 41 (2023) 521–531.
[27] X. Li, J. Jin, W. Xu, M. Wang, L. Liu, Abortive ligation intermediate blocks seamless repair of double-stranded breaks, Int. J. Biol. Macromol. 209 (2022) 1498–1503.
[28] A. Yang, J. Cheng, M. Liu, Y. Shangguan, L. Liu, Sandwich fusion of CBM9_2 to enhance xylanase thermostability and activity, Int. J. Biol. Macromol. 117 (2018) 586–591.
[29] Y. Liang, Y. Zhang, L. Liu, Intra-molecular homologous recombination of scarless plasmid, Int. J. Mol. Sci. 21 (2020) 1697.
[30] J. Howard, J. Ward, J.N. Watson, K.H. Roux, Heteroduplex cleavage analysis using S1 nuclease, Biotechniques 27 (1999) 18–19.
[31] S. Verma, F. Eckstein, Modified oligonucleotides: synthesis and strategy for users, Annu. Rev. Biochem. 67 (1998) 99–134.
[32] X. Liu, J.H. Liu, The terminal 5' phosphate and proximate phosphorothioate promote ligation-independent cloning, Protein Sci. 19 (2010) 967–973.
[33] Q. Huang, J. Li, T. Shi, J. Liang, Z. Wang, L. Bai, Z. Deng, Y. Zhao, Defense mechanism of phosphorothioated DNA under peroxynitrite-mediated oxidative stress, ACS Chem. Biol. 15 (2020) 2558–2567.
[34] J. Zhang, X. Xing, A.B. Herr, C.E. Bell, Crystal structure of *E.coli* RecE protein reveals a toroidal tetramer for processing double-stranded DNA breaks, Structure 17 (2009) 690–702.
[35] G. Tolun, R.S. Myers, A real-time DNase assay (ReDA) based on PicoGreen fluorescence, Nucleic Acids Res. 31 (2003) e111.
[36] T. Perkins, R.V. Dalal, P.G. Mitsis, S.M. Block, Sequence dependent pausing of single lambda exonuclease molecules, Science 301 (2003) 1914–1918.
[37] J. Kypr, I. Kejnovská, D. Renciuk, M. Vorlícková, Circular dichroism and conformational polymorphism of DNA, Nucleic Acids Res. 37 (2009) 1713–1725.
[38] B. Ranjbar, P. Gill, Circular dichroism techniques: biomolecular and nanostructural analyses- a review, Chem. Biol. Drug Des. 74 (2009) 101–120.
[39] H. Jaganathan, A. Ivanisevic, Circular dichroism study of enzymatic manipulation on magnetic and metallic DNA template nanowires, Colloids Surf., B 67 (2) (2008) 279–283.
[40] L. Wang, S. Chen, K.L. Vergin, S.J. Giovannoni, S.W. Chan, M.S. DeMott, K. Taghizadeh, O.X. Cordero, M. Cutler, S. Timberlake, E.J. Alm, M.F. Polz, J. Pinhassi, Z.X. Deng, P.C. Dedon, DNA phosphorothioation is widespread and quantized in bacterial genomes, Proc. Natl. Acad. Sci. U. S. A 108 (2011) 2963–2968.
[41] B.J. Caldwell, E. Zakharova, G.T. Filsinger, T.M. Wannier, J.P. Hempfling, L. Chun-Der, D. Pei, G.M. Church, C.E. Bell, Crystal structure of the Redβ C-terminal domain in complex with λ Exonuclease reveals an unexpected homology with λ Orf and an interaction with *Escherichia coli* single stranded DNA binding protein, Nucleic Acids Res. 47 (2019) 1950–1963.
[42] B. Caldwell, A. Norris, C. Karbowski, A. Wiegand, V. Wysocki, C. Bell, Structure of a RecT/Redβ family recombinase in complex with a duplex intermediate of DNA annealing, Nat. Commun. 13 (2022) 7855.
[43] E. Lin, Y. Huang, R. Luo, Z. Basharat, C. Huang, Crystal structure of an SSB protein from *Salmonella enterica* and its inhibition by *Flavanonol* taxifolin, Int. J. Mol. Sci. 23 (2022) 4399.